

## MHD simulation on ablation cloud in tokamak and heliotron

R. Ishizaki 1), N. Nakajima 1) and M. Okamoto 2)

1) National Institute for Fusion Science, 322-6 Oroshi-cho, Toki, Gifu 509-5292, Japan

2) Chubu University, 1200 Matsumoto-cho, Kasugai, Aichi 487-8501, Japan

e-mail contact of main author : ishizaki@nifs.ac.jp

**Abstract.** It is well known that an ablation cloud drifts to the lower field side in tokamak plasmas, which leads to a good performance on fueling in tokamak. Such a good performance, however, has not been obtained yet in the planar axis heliotron; Large Helical Device (LHD) experiments, even if a pellet has been injected from the high field side. The purpose of the study is to clarify the difference on the cloud motion between tokamak and LHD plasmas by using the MHD simulation including ablation processes. It is found in tokamaks that the drift motion is induced by a tire tube force and  $1/R$  force in the major radius direction, and that the pressure and density of the plasmoid have oscillation due to fast compressional Alfvén wave. The first trial simulations on the motion of the plasmoid in a straight helical and LHD plasmas also show that the plasmoid drifts to the lower field side similarly to tokamaks. However, an plasmoid drifts inward or outward of the flux surfaces depending on the location along the magnetic field lines, since the plasmoid expands along the magnetic field with time, the magnetic field strength and the direction of the magnetic curvature change along the magnetic field lines due to both toroidicity and helicity of the helical coils, and the rotational transform is greater than that in tokamaks in the plasma periphery. Thus, it is suggested that the difference of the pellet injections between the high field and the low field sides is reduced in helical plasmas.

### 1. Introduction

Injecting small pellets of frozen hydrogen into torus plasmas is a proven method of fueling [1]. The physical processes are divided into the following micro and macro stages. The micro stage is the ablation of mass at the pellet surface due to the high temperature bulk plasma which the pellet encounters. The neutral gas produced by the ablation is rapidly heated by electrons and ionized to form a high density and low temperature plasma, namely a plasmoid. The macro stage is the redistribution of the plasmoid by free streaming along the magnetic field lines and by MHD processes which cause mass flow across flux surfaces. The micro stage is well-understood by an analytic method [2] and numerical simulation [3]. The drift motion of the plasmoid is investigated in the macro stage [4]. Since the plasmoid drifts to the lower field side, the pellet fueling to make the plasmoid approach the core plasma has succeeded by injecting the pellet from the high field side in tokamak. On the other hand, such a pellet fueling has not succeeded in LHD plasmas for various injection locations, say, even if the pellet is injected from the high field side [5].

The purpose of the study is to clarify the difference on the motion of the plasmoid between tokamak and helical plasmas. In order to investigate the motion of the plasmoid, the three dimensional MHD code including the ablation processes has been developed by extending the pellet ablation code (CAP) [3]. It is found through the comparison between simulation results and an analytical consideration that the drift motion to the lower field side in tokamak is induced by a tire tube force due to the extremely large pressure of the plasmoid and a  $1/R$  force due to

the magnetic pressure gradient and curvature in the major radius direction. It is also found that the plasmoid dose not drift when the perturbation of the plasmoid is small. The motion of the plasmoid is investigated in a straight helical and toroidal LHD plasmas in an initial short time, from which it is found out that the plasmod drifts to the lower field side as well as in tokamaks. Consequently, the common mechanism is considered to work between tokamaks and helical configurations. However, the directions of the magnetic curvature and gradient of the magnetic field strength in the helical configurations are completely different from those of tokamaks due to the helicity of the helical coils, which leads to the difference of the experimental results between tokamaks and helical configurations.

## 2. Basic Equations

Since the plasmoid is such a large perturbation that the linear theory can not be applied, a nonlinear simulation is required to clarify the behavior of the plasmoid. The drift motion is considered to be a MHD behavior because the drift speed obtained from experimental data [1] is about  $0.01 \sim 1.0v_A$ , where  $v_A$  is an Alfvén velocity. Thus, the three dimensional MHD code including the ablation processes has been developed by extending the pellet ablation code (CAP) [3]. The equations used in code are:

$$\frac{d\rho}{dt} = -\rho \nabla \cdot \mathbf{u}, \quad (1a)$$

$$\rho \frac{d\mathbf{u}}{dt} = -\frac{\beta}{2} \nabla p + (\nabla \times \mathbf{B}) \times \mathbf{B}, \quad (1b)$$

$$\frac{dp}{dt} = -\gamma p \nabla \cdot \mathbf{u} + H, \quad (1c)$$

$$\frac{\partial \mathbf{B}}{\partial t} = \nabla \times (\mathbf{u} \times \mathbf{B}) \quad (1d)$$

All variables except time and length are normalized by ones at the magnetic axis,  $\rho_0$ ,  $p_0$ ,  $B_0$  and  $v_A$ , where  $v_A = B_0/\sqrt{\mu_0\rho_0}$ . Length and time are normalized by the major radius at the center of the poloidal surface,  $R_0$ , and Alfvén transit time,  $\tau_A = R_0/v_A$ , respectively.  $\gamma$  and  $\beta = 2\mu_0 p_0/B_0^2$  are the ratio of the specific heats and plasma beta, respectively. Heat source  $H$  is given by:

$$H = \frac{dq_+}{dl} + \frac{dq_-}{dl}. \quad (2)$$

where  $q_{\pm}$  is the heat flux model dependent on electron density and temperature in the bulk plasma and the plasmoid density.  $l$  is the distance along the field line. The subscript  $+$  ( $-$ ) refers to the right (left)-going electrons. Then, the heat source can be calculated on each field line. Assuming Maxwellian electrons incident to the plasmoid, a kinetic treatment using a collisional stopping power formula leads to the heat flux model,  $q_{\pm}$  [3] which is used in construction of one of the ablation models [2]. In the tokamak simulations, the cylindrical coordinate system is used, and the rotational helical coordinate system is used in the helical calculations as shown in Ref. [6]. The boundary is assumed to be a perfect conductor. The Cubic Interpolated Pseudoparticle (CIP) method is used in the code as a numerical scheme [7].

### 3. Plasmoid simulations in Tokamak

MHD simulation has been carried out to clarify an essence of drift motion of the plasmoid in tokamak plasma with  $\beta = 0.01$  and  $R/a = 2$  as shown in Fig. 1, where  $\beta$  is the plasma beta, and  $R$  and  $a$  are major and minor radii, respectively. In an initial condition, a plasmoid is located at the center of the poloidal cross section as shown in Fig. 1, and peak values of density and temperature of the plasmoid are 1000 times density and 1/1000 times temperature of the bulk plasma at the magnetic axis, respectively. The plasmoid, whose half width is  $0.03R$ , encounters the electrons with fixed temperature 2 keV and density  $10^{20} \text{ m}^{-3}$ . Figures 2(a) and (b) show density contours in the equatorial plane at  $t = 1.0$  and  $6.0\tau_A$ , respectively. The plasmoid is found to expand in the toroidal direction and simultaneously drifts to the lower field side. Figure 3 shows temporal evolution of peak values of the plasmoid pressure and density. The pressure reaches more than 150 times the bulk plasma pressure due to heating. On the other hand, the density decreases because the plasmoid expands along the magnetic field. Since decrease in the density reduces the energy deposit to the plasmoid, the pressure decreases after it reaches a peak value. In addition, the pressure and density have oscillation with a period of about  $1.0\tau_A$  induced by the fast compressional Alfvén wave.

In order to evaluate a force inducing drift motion of a plasmoid in torus plasmas, we assume the following three conditions. (1) The bulk plasma is an uniform plasma with a vacuum toroidal magnetic field. (2) A plasmoid is given by pressure perturbation  $\Delta p$ , density perturbation  $\Delta \rho$  and magnetic field perturbation  $\Delta B^2$  without heat source  $H$  in Eq.(1c). Although  $\Delta p$  and  $\Delta \rho$  have positive values,  $\Delta B^2$  has a negative value because the magnetic field is reduced by a diamagnetic current. (3) Physical quantities are uniform in toroidal direction. Integrating the Eq. (1b) over the plasmoid volume, one can obtain an analytical formula on the acceleration in the major radius direction:

$$\alpha = \frac{du_R}{dt} = \frac{\Delta(\beta p/2) - \Delta(B^2/2)}{\rho R}, \quad (3)$$

where  $u_R$  is velocity of the plasmoid in the direction of the major radius. The first term in the right hand side expresses a tire tube force induced by the plasmoid pressure. The second term in it expresses a  $1/R$  force in the major radius direction induced by the magnetic pressure gradient and curvature. Both forces make  $\alpha$  increase because  $\Delta(\beta p/2)$  and  $\Delta(B^2/2)$  are positive and negative, respectively. Assuming those absolute values are comparable, one obtains:  $\alpha \sim \beta \Delta p / \rho R$ . The fact that the acceleration is proportional to  $1/R$  means that the curvature of the magnetic field is one essence of the drift motion. The simulations have been carried out in the above three conditions. Note that the directions of the magnetic curvature and the gradient of the main magnetic field strength are in the major radius direction. Figure 4 shows the displacement in the major radius of the plasmoid with time. The displacement is normalized by an initial acceleration;  $\alpha_0$ . A thin solid line shows  $\Delta R / (\alpha_0/2) = t^2$  which means the motion with a constant acceleration;  $\alpha_0$ . It is found that the normalized simulation results agree with the analytical formula in  $t > 10$ . However, since  $\Delta p$  decreases and  $R$  increases due to the drift motion of the plasmoid, the acceleration shown by Eq. (3) is reduced. Thus, the simulation results are found to be slightly saturated with time. Subsequently, the plasmoid stops because it reaches the boundary, namely the perfect conductor. Simulation results have the shape of stairs because the coordinates with the grid points are used as the displacement of the plasmoid. In

result, it is found that the drift motion of the plasmoid is induced by the tire tube force and  $1/R$  force in the major radius direction. Although the result is obtained under the restricted conditions as shown above, the essence of the drift motion is considered to be same in the case that the pressure is induced by the heat source and the plasmoid expands along the magnetic field. There is another essential physics in Fig. 4. Only simulation indicated by 3400 dose not agree with the analytical line. Since the perturbations are small in this case, the linear theory is applicable to it unlike the other data. The linear theory predicts that the perturbation has just oscillation in stable equilibrium plasmas. Thus, small perturbations do not have the drift motion. In other words, a large perturbation violating linear theory is another essence of the drift motion.

#### 4. Plasmoid simulations in straight helical and toroidal LHD

The motion of a plasmoid is investigated in a straight helical system consisting of uniform bulk pressure and a vacuum magnetic field. The plasmoid is assumed to be an initial pressure and density perturbations with helical symmetry, which has 10 times pressure and 1000 times density of the bulk plasma without heating source  $H$  in Eq.(1C). Figures 5(a) and (b) show contours of magnetic surface and magnetic pressure in the bulk plasma. Locations of initial perturbations are shown by circles which are at (a) lower field side and (b) higher field side than that at the magnetic axis. Figures 5(c) and (d) show temporal evolutions of the density profiles for (a) and (b), respectively. When the plasmoid drifts, density gradient ahead of it becomes steep in general. Then, it is found that the plasmoid drifts outward in (c) and inward in (d) as shown by arrows. In other words, the plasmoid drifts to the lower field side in both cases. That fact is consistent with the result in tokamaks. Figure 6 shows temporal evolution of the peak values of the pressure and density in Fig. 5(a). It is found that both the pressure and density monotonously decrease. A similar result is obtained for case in Fig. 5(b).

The motion of the plasmoid is also evaluated in toroidal LHD plasma. An initial condition of the plasmoid and heating condition are similar to ones in Sec. 3. Figures 7(a) and (b) show contours of plasma and magnetic pressures in different poloidal cross sections in LHD. Initial locations of the plasmoids are shown by circles indicated by A, B, C and D. The plasmoid indicated by A and C are located at the inner side of the torus, and those denoted by B and D are located at the outer side of it. Figure 8 shows velocities at the peak densities of the plasmoids. The plasmoids for A and D drift in the positive direction of the major radius. The plasmoid for C drifts in the negative direction of it and that for B hardly drifts. It is found that the plasmoids for A, C and D drift to the lower field side when it refers to the contour of the magnetic pressure shown in Fig. 7. The plasmoid for B dose not drift in the direction of the major radius where the magnetic pressure is almost at a saddle point. Therefore, physics mechanism that the plasmoid drifts to the lower field side is common among tokamak, straight helical and toroidal LHD. However, in helical plasmas, since (1) the distribution of magnetic field strength and the direction of the magnetic curvature change by both toroidicity as well as in tokamaks and helicity due to helical coils along the magnetic field lines and (2) the rotational transform becomes large in the plasma periphery, the plasmoid drifts inward or outward of the flux surfaces depending on the location. Thus, the difference between Figs. 5(c) and (d) may be reduced in the straight helical. In LHD, when the plasmoid density is integrated along the magnetic field lines, the difference of the velocity in the direction of the major radius as shown

in Fig. 8 may be reduced. This expectation seems to be consistent with the fact that there is no difference between the density profiles obtained by the pellet injections from various locations in LHD experiments.

## 5. Summary and Discussion

It is verified by simulations using the CAP code that the plasmoid with a high pressure induced by heat flux drifts to the lower field side in both tokamak and helical configurations. It is found out through comparison between simulations and analytical treatment that the such the drift is due to a tire tube force coming from a extremely large pressure of the plasmoid and  $1/R$  force of magnetic curvature. It is shown that the plasmoid dose not drift but oscillates when its pressure perturbation is small, and that such a high pressure excites the fast compressional Alfvén wave. The differences of experimental results of the plasmoid motions between tokamaks and helical configurations are considered to come from the differences of the magnetic configurations of the bulk plasma. In the helical configurations, the magnetic field strength and the magnetic curvature are affected by both toroidicity and helicity of helical coils, which leads to the inward and outward drift of the plasmoid along the magnetic field lines. In order to confirm such an interpretation and to seek the ways obtaining good performance, long time simulations in the helical plasmas will be performed.

## Acknowledgments

The authors thank Prof. Sudo for his encouragement. One of the authors R. I. is supported by the Japanese Ministry of Education, Culture, Sports, Science, and Technology, Grant No. 15560719.

## References

- [1] H. W. Müller *et al*, Nucl. Fusion **42**, 301 (2002).
- [2] Parks, P. B. & Rosenbluth, M. N. Phys. Plasmas **5**, 1380 (1998).
- [3] R. Ishizaki *et al*, Phys. Plasmas **11**, 4064 (2004).
- [4] P. B. Parks, Phys. Rev. Lett. **94**, 125002 (2005).
- [5] R. Sakamoto, in proceedings of 29th EPS conference on Plasma Phys. and Control. Fusion.
- [6] K. Harafuji *et al*, J. Comp. Phys. **81**, 169 (1989).
- [7] H. Takewaki *et al* J. Comput. Phys. **61**, 261 (1985).

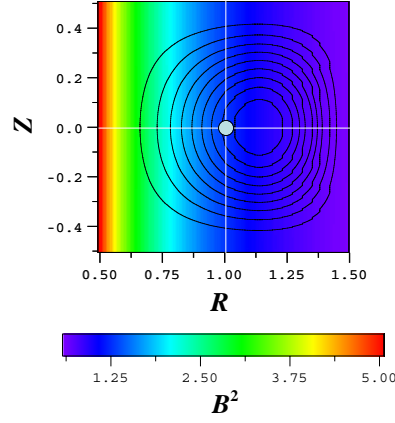


FIG. 1: *Initial location of the plasmoid on the poloidal surface in tokamak where contours of plasma and magnetic pressures are shown by lines and color, respectively.*

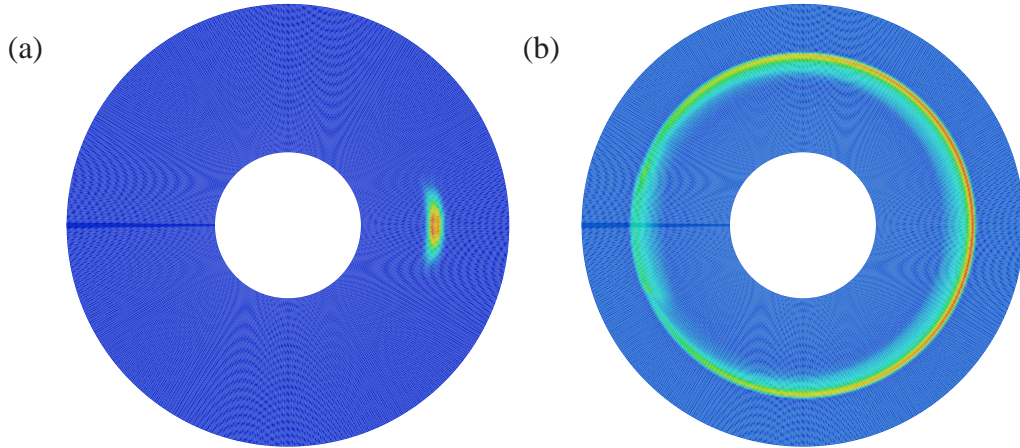


FIG. 2: *Density contours in the equatorial plane in tokamak at (a)  $t = 1.0\tau_A$  and (b)  $t = 6.0\tau_A$ .*

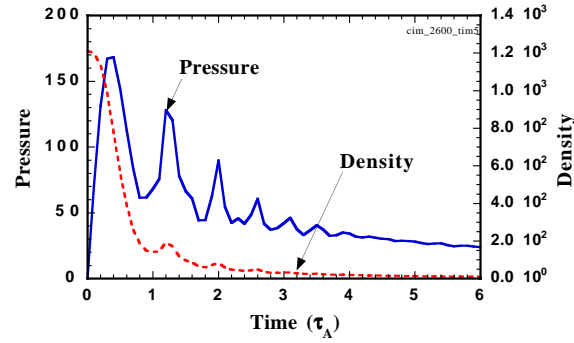


FIG. 3: *Peak values of pressure (solid line) and density (dashed line) of the plasmoid vs. time. for Fig. 2*



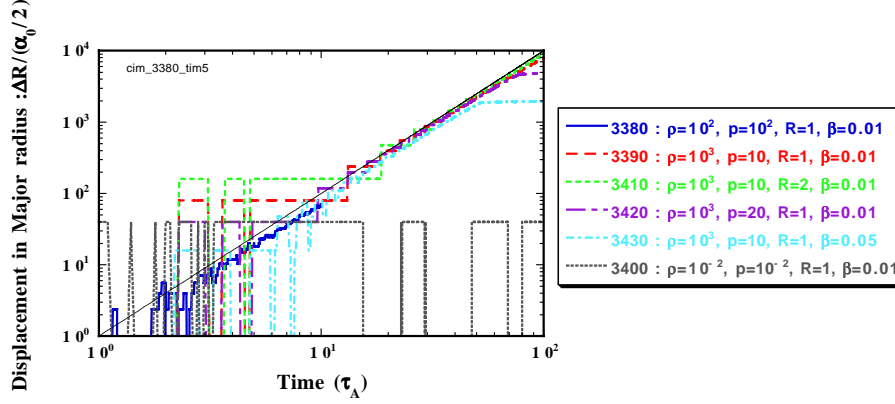


FIG. 4: Normalized displacement in the major radius of the plasmoid vs. time in uniform plasmas with the toroidal magnetic fields.  $\Delta\rho$  and  $\Delta p$  are density and pressure perturbations.  $R$  is an initial location in the major radius.  $\beta$  is the plasma beta in the bulk plasma. A thin solid line shows  $\Delta R/(\alpha_0/2) = t^2$ .

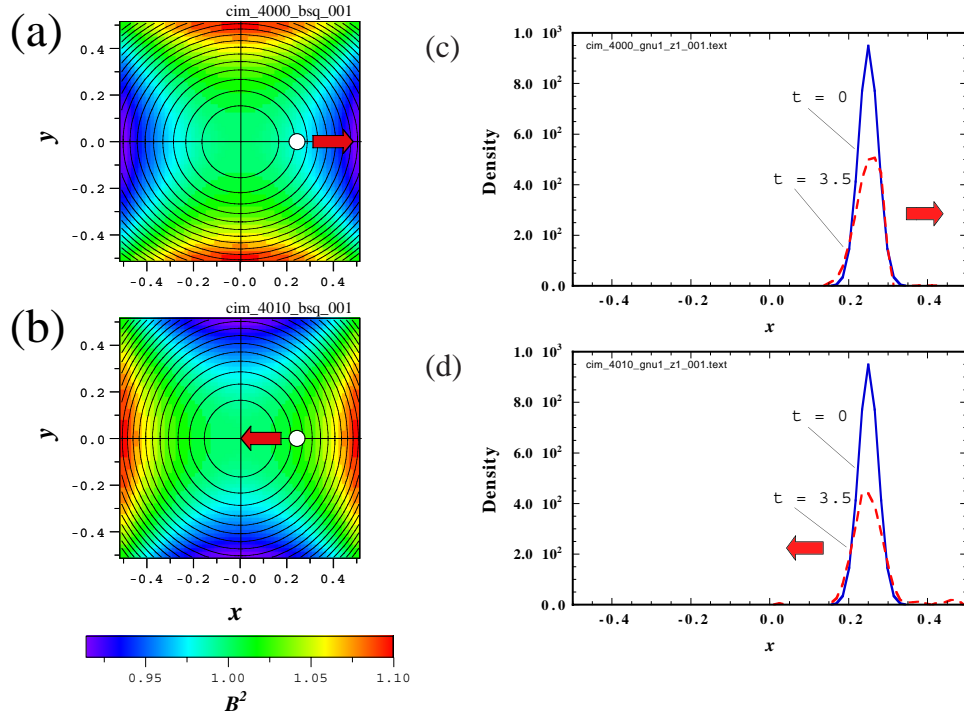


FIG. 5: Initial locations of the plasmoids at (a) lower field side and (b) higher field side than one at the magnetic axis in two different poloidal surfaces in straight helical plasma, where contours of magnetic surfaces and magnetic pressures are shown by lines and color, respectively. Density profiles (c) for (a), and (d) for (b), at  $t = 0$  (solid line) and  $3.5\tau_A$  (dashed line).

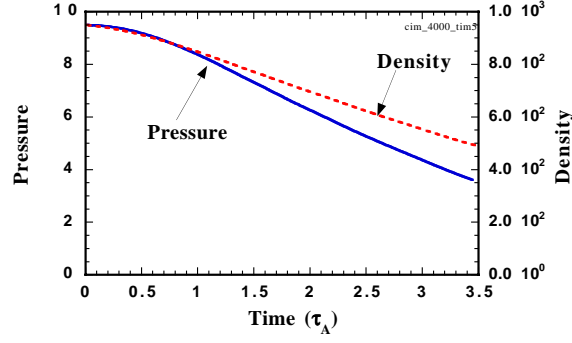


FIG. 6: Peak values of pressure (solid line) and density (dashed line) of the plasmoid vs. time for Fig. 5(a).

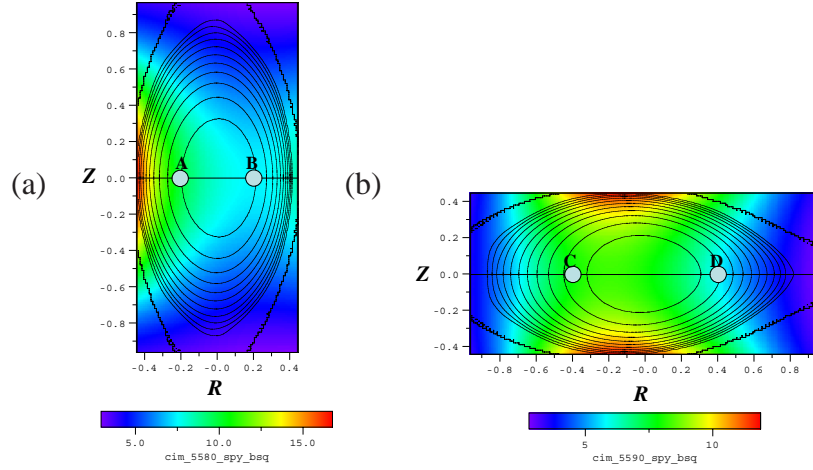


FIG. 7: Initial locations of the plasmoids at the inside (A, C) and the outside (B, D) of the torus in two different poloidal surfaces, (a) and (b) in LHD, where contours of plasma and magnetic pressures are shown by lines and color, respectively.

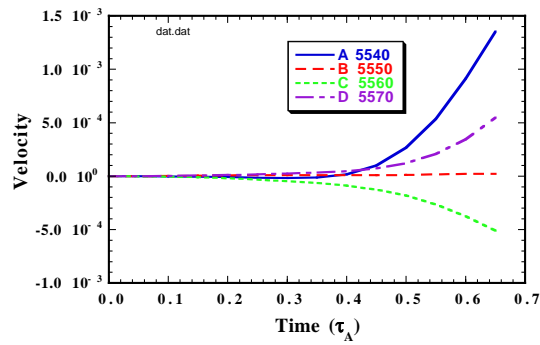


FIG. 8: Velocities at the peak densities of the plasmoids A, B, C and D in Fig. 7.